ELSEVIER

Journal of Photochemistry and Photobiology A: Chemistry 121 (1999) 91–97

Journal of Photochemistry and Photobiology A:Chemistry

Luminescence studies of benzamide derivatives at room and low temperatures

Józef Heldt[a,b], Janina R. Heldt[b,*], Elżbieta Szatan[b]

[a]*Institute of Physics, Pedagogical University at Słupsk, ul.Arciszewskiego 22, Słupsk 76-200, Poland*
[b]*Institute of Experimental Physics, University of Gdańsk, ul.Wita Stwosza 57, Gdańsk 80-952, Poland*

Received 2 July 1998; received in revised form 9 July 1998; accepted 18 November 1998

Abstract

In this study the luminescence spectra and fluorescence decay times of benzamide and its three derivatives have been measured at room and low temperatures in MCH, EPA and IP/EE mixtures. The bichromophoric derivatives i.e., *N*-phenylbenzamide and *N*,*N*′-methylphenylbenzamide yield dual fluorescence. The phosphorescence spectra of the molecules under study show a blue shift when non-polar rigid solvent is replaced with polar one. This effect, and the same λ_{max} values of the phosphorescence bands indicate that the phosphorescence emissions originate from the (n, π^*) state of the benzoic moiety. The small τ values of the S_1(LE) state suggest that the rate constants of the excited state proton-transfer tautomer and TICT isomer creation processes are large. The τ values of molecules in the S_1(LE), S_1'(PT), and S_1''(CT) states differ significantly.

Keywords: Benzamides; Absorption and emission spectra; Fluorescence decay time; PACS: 3350 D

1. Introduction

In the last years benzamide derivatives have been studied for various aspects [1–12]. From the luminescence studies it follows that the fluorescence spectra of some benzamide derivatives e.g., *N*-phenylbenzamide exhibits two bands: F_1(LE) ascribed to the normal S_1(LE) → S_0 fluorescence, and the F_2 band recognised as comprising the F_2'(PT) and the F_2''(CT) emissions which stem from proton-transfer tautomers S_1'(PT) → S_0'(PT), and twisted intramolecular charge-transfer isomers S_1''(CT) → S_0(FC), respectively [8–16].

Azumaya et al. [17] on the grounds of fluorescence decay time measurements at 300 K for a number of aromatic anilides have concluded that the F_2 emission band is generated by the S_1 state of twisted intramolecular charge-transfer (TICT) species only. According to them the twisting motion takes place around the amide N–CO bond. Furthermore, they have shown that fixation of the Ar–CO and N–CO bonds achieved by substitution of steric hindrance (methyl group's) results in the absence of the F_2 emission. This hypothesis was proved by fluorescence spectra studies of inflexible aromatic anilides e.g., *N*-phenylisoindolinone. Those findings made them rule out radiation originating from the imidol form of benzanilide created in a photo-induced excited-state double proton-transfer reaction. This is in contradiction to what Tang et al. [8] suggested that the imidol form of benzanilide is responsible for the F_2 emission. For benzamide and its bichromophoric derivatives in rigid solutions the twisting motions around amide N–CO and around the Ar–CO and Ar–N bonds are restricted. According to Azumaya et al. [17] in such conditions the F_2 radiation should disappear and instead of the F_2 emission (observed at 300 K) a new fluorescence band should appear.

It was very tempting to perform necessary luminescence studies at low temperature, which would verify the suggestions made in I. Azumaya et al. [17]. Our studies include comparative research of the absorption and emission spectra as well as the fluorescence decay times (obtained at different emission wavelengths) of benzamide (**I**), *N*-methylbenzamide (**II**), *N*-phenylbenzamide (**III**), and *N*,*N*′-methylphenylbenzamide (**IV**). The measurements have been performed both at room (296 K) and low (168 and 77 K) temperatures in polar and non-polar solvents. The results obtained have allowed to distinguish discrete fluorescence de-excitation pathways as well as verify the suggestion concerning the influence of intramolecular motions on appearance or absence of the F_2 fluorescence emission band.

*Corresponding author. E-mail: fizjh@univ.gda.pl

1010-6030/99/$ – see front matter
PII: S1010-6030(98)00442-0

2. Experimental section

Absorption spectra measurements were carried out by using a Shimadzu UV-2100 recording spectrophotometer fitted with a rectangular suprasil absorption cell. Luminescence spectra were obtained using a SFR-100 ratio recording spectrofluorimeter equipped with a standard or modified sample compartment for room and low temperature measurements, respectively. Luminescence was observed perpendicularly to the direction of the exciting beam from a square suprasil 10 mm cell (measurements at 296 K) or from a 2 mm in diameter quartz tube, which was placed in a vacuum-sealed quartz finger Dewar flask containing liquid nitrogen. Phosphorescence spectra was recorded by the same apparatus with a mechanical chopper performing as a phosphoroscope added. The compounds under study are shown in

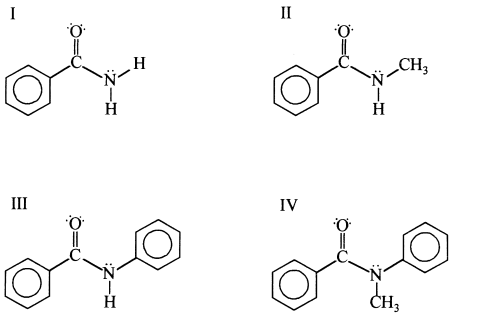

I benzamide **II** N-methylbenzamide
III N-phenylbenzamide **IV** N,N'-methylphenylbenzamide

The concentration of the solutions was 2×10^{-4} M.

The fluorescence decay times of the molecules in question have been determined by using a BESSY synchrotron radiation for excitation [18], as well as by means of a streak camera single mode-locked Nd:YAG picosecond laser emission spectrometer [19]. When the former equipment was used, the decay of the fluorescence emission of **III** and **IV** was detected at different wavelengths of the F_2 band using standard photon-counting equipment. Apart from that, the decay time of the total F_2 fluorescence bands of the molecules under study were measured using the latter set-up. In this case the fluorescence light excited by the fourth harmonic of the Nd : YAG laser was detected with a Hamamatsu model C979–01 streak camera connected to a two dimensional silicon intensified-target (SIT) detector. The output from this detector was digitised for data analysis by an IBM PC computer. Selecting of the emission bands (F_1 or F_2 band) was accomplished using different Coring Glass Filters. The fluorescence decay time measurements were performed at room (296 K) and low (168 and 77 K) temperatures in deaerated MCH, EPA (ethyl ether : isopentane: ethanol = 5 : 5 : 2 v/v), and IP/EE (isopentane : ethyl ether = 1 : 1 v/v) solutions. The experimental data of the fluorescence decay curves were fitted by the iterative deconvolution technique (the Marquardt–Levenberg algorithm) to mono- or bi-exponential model function.

3. Absorption, fluorescence and phosphorescence spectra

The absorption spectra of the molecules dissolved in methylcyclohexane (MCH) at room temperature are shown in Fig. 1. The absorption spectra of benzamide and *N*-methylbenzamide in the region of 200–300 nm have two distinct bands: a strong band around 230 nm ($\varepsilon \cong 11\,000$ $M^{-1}\,cm^{-1}$) and a very weak one at about 270 nm ($\varepsilon \cong 800$ $M^{-1}\,cm^{-1}$). This weak band has its oscillation structure with a wavenumber difference of about 1200 cm^{-1} between the adjacent peaks. This band has a (n, π^*) character. The shape of the absorption spectrum of **III** differs from that of **I**. It consists of three bands [14–16]: one at 215 nm, another at 260 nm ($\varepsilon = 12\,700$ $M^{-1}\,cm^{-1}$) and the third, a very weak ($\varepsilon \cong 500$ $M^{-1}\,cm^{-1}$) (n, π^*) absorption band at 305 nm. The last band is overlapped by the second one, however, its existence has been revealed by the fluorescence excitation spectra [15]. These absorption peaks are more clearly seen in the spectra where absorption pathway is longer (Fig. 1(a) and Fig. 1(c)). For molecule **IV**, the band equivalent to that at 215 nm is shifted to a longer wavelength whereas the positions of the two other bands remain unchanged. This leads to formation of the unstructured spectrum (Fig. 1(d)). The determined peak values of the absorption bands agree well with the results of the quantum mechanical calculations performed by Belotsvetov et al. [1] and Kosobutskii et al. [2].

Fig. 2 shows the luminescence spectra of compounds **I** and **II** in MCH and EPA glasses at 77 K. The total luminescence spectra of **I** and **II** (solid lines) yield two peaks: one,

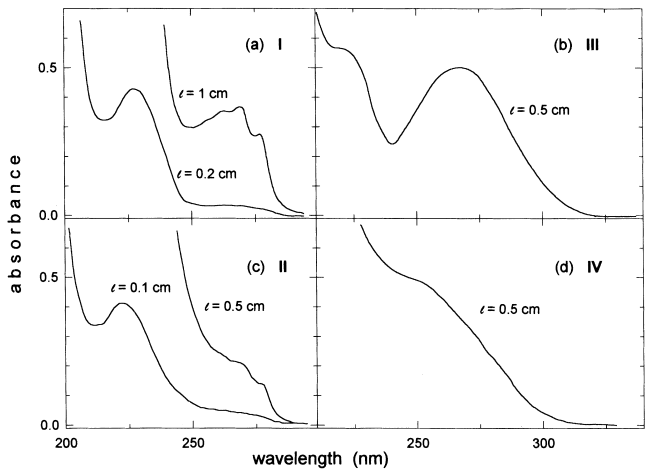

Fig. 1. The absorption spectra of (a) benzamide, (b) *N*-phenylbenzamide, (c) *N*-methylbenzamide, (d) *N,N'*-methylphenylbenzamide in deaerated and dehydrated methycyclohexane at 296 K. 1 –absorpion pathway; concentration $c = 2 \times 10^{-4}$ M

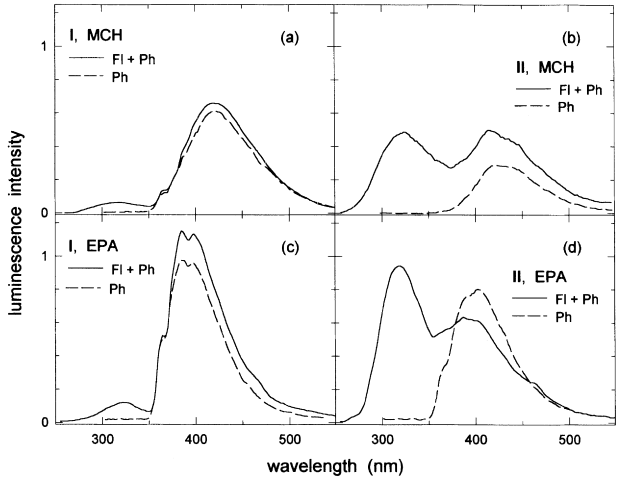

Fig. 2. The total luminescence and phosphorescence spectra of benzamide (**I**) and *N*-methylbenzamide (**II**) in MCH and EPA glasses at 77 K. Concentration $c = 2 \times 10^{-4}$ M

attributed to the normal $S_1(LE) \rightarrow S_0$ fluorescence and the second, ascribed to the $T_1(LE) \rightarrow S_0$ phosphorescence emission. The intensity of the phosphorescence band of **I** (dashed lines) is by one order of magnitude greater than the $F_1(LE)$ fluorescence band. The phosphorescence spectra of **I** and **II** in EPA glasses show distinct oscillation structure which is more noticeable in **I** than in **II**. The maximum wavelength of the phosphorescence band of **I** and **II** increases from 395 to 425 nm and from 405 to 430 nm, respectively, if the solvent is changed from EPA to MCH.

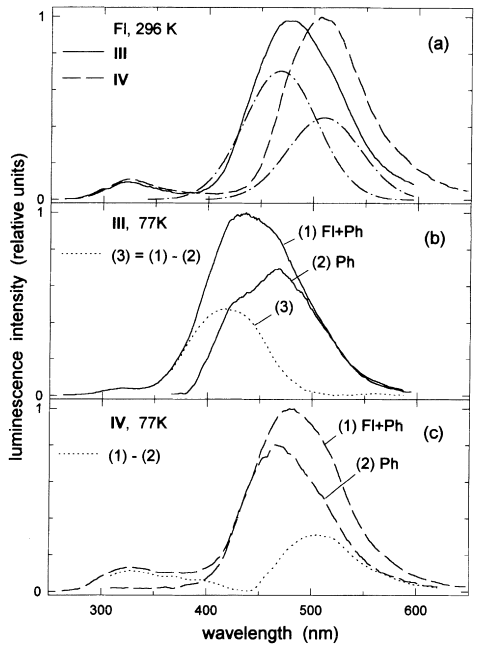

Fig. 3. *N*-phenylbenzamide (**III**) and *N*,*N*′-methylphenylbenzamide (**IV**) in MCH: (a) the fluorescence spectra at 296 K; the dash-dot lines show the decompositon of the F_2 band of **III**, (b) the total luminescence and the phosphorescence spectra of **III** at 77 K, (c) the total luminescence and the phosphorescence spectra of **IV** at 77 K. Concentration $c = 2 \times 10^{-4}$ M.

Fig. 3 shows the luminescence spectra of **III** and **IV** in MCH at 296 K as well as in rigid solutions at 77 K. Panel a of Fig. 3 shows the fluorescence spectra of these two molecules obtained at 296 K in MCH. The spectrum of **III** has two bands, respectively, assigned as a weak $F_1(LE)$ band with λ_{max} at 325 nm and a stronger F_2 band ($\lambda_{max} = 478$ nm). The F_2 band as suggested [14–16], consists of two independent emissions: a proton-transfer band, $F_2'(PT)$ ($\lambda_{max} = 468$ nm) and a charge-transfer band, $F_2''(CT)$ ($\lambda_{max} = 510$ nm) for which the ratio of their intensities equal to 0.61 : 0.39. The two components of the F_2 band are plotted as dash-dot lines (see Fig. 3(a)). Panels b and c show the total emission spectra i.e., the combined fluorescence and phosphorescence radiation as well as the pure phosphorescence bands of **III** and **IV** in MCH at 77 K. In Fig. 4 there are equivalent spectra in EPA and IP/EE glasses. The curves in these figures are labelled (1) and (2), respectively. Comparing the spectra presented in Figs. 3 and 4 it may be noticed that at 77 K the intensity of a normal $F_1(LE)$ fluorescence band depends on the kind of the solvent used. It is greater in polar (EPA, IP/EE) than in non-polar frozen glasses (MCH). It must be pointed out that long-wavelength bands in the total emission spectra of **III** and **IV** (curves (1)) differ from those of the pure phosphorescence spectrum (curves (2)). Moreover, the F_2 fluorescence bands of these two compounds at 296 K show a pronounced anomaly i.e., the F_2 fluorescence band has its maximum at a longer wavelength than the phosphorescence band, $\lambda_{max}(F_2) > \lambda_{max}(Ph)$, (Figs. 3 and 4(c) and Fig. 4(d)). It is also distinctive, that in EPA and IP/EE glasses for **III** $\lambda_{max}(Fl + Ph) > \lambda_{max}(Ph)$, whereas in MCH the opposite inequality is true i.e., $\lambda_{max}(Fl + Ph) < \lambda_{max}(Ph)$ (Fig. 3(b)).

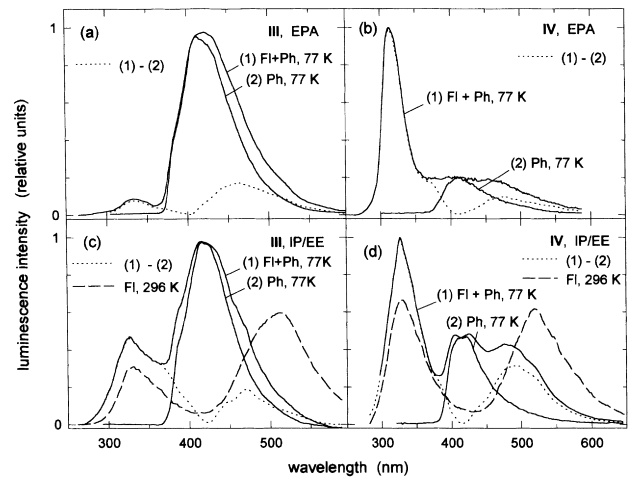

Fig. 4. *N*-phenylbenzamide (**III**) and *N*,*N*′-methylphenylbenzamide (**IV**) in EPA and IP/EE: (a) the total luminescence and the phosphorescence spectra of **III** in EPA at 77 K, (b) the total luminescence and the phosphorescence spectra of **IV** in EPA at 77 K, (c) the total luminescence and the phosphorescence spectra of **III** in IP/EE at 77 K, and fluorescence at 296 K, (d) the total luminescence and the phosphorescence spectra of **IV** in IP/EE at 77 K, and fluorescence at 296 K. Concentration $c = 2 \times 10^{-4}$ M.

In the case of **III** dissolved in MCH such wavelength dependence is comprehensible if one assumes that at 77 K a new emission band appears with its maximum around 420 nm. The contour of this band has been drawn after subtracting the pure phosphorescence spectrum from the normalised contour of the total luminescence, see dotted curve (3) in Fig. 3(b). It is supposed that this band results from the emission of dipolar aggregates of **III** [8,20]. At the long-wavelength region of the spectra of **IV** the inequality $\lambda_{max}(Fl + Ph) > \lambda_{max}(Ph)$ is valid for all the rigid solutions used (Fig. 3(c), Fig. 4(b) and Fig. 4(d)). This band is the sum of a pure phosphorescence band and a weak $F_2''(CT)$ band. The dotted curves in Fig. 3 and Fig. 4 plot the result of subtraction the phosphorescence spectra from the total emission spectra. The F_2'' (CT) band has the highest intensity in IP/EE rigid solutions.

The above low temperature spectroscopic studies of **III** and **IV** lead one to conclude that

- in MCH at 77 K the total luminescence spectrum of **III** consists of a very weak F_1(LE) band (onset 290 nm, $\lambda_{max} = 314$ nm), a weak fluorescence band of *N*-phenylbenzamide aggregates (Fig. 3(b), curve (3), onset 350 nm, $\lambda_{max} = 420$ nm) and the phosphorescence band with λ_{max} at 460 nm; neither F_2'(PT) nor F_2''(CT) emission is observed;
- in polar solvents e.g., in EPA and IP/EE glasses the normal F_1(LE) fluorescence band is shifted to a longer wavelength, $\lambda_{max} \cong 330$ nm, whereas the phosphorescence band is shifted to a shorter wavelength and its maximum is around 415 nm;
- luminescence spectra of **IV** consist of F_1(LE), Ph and F_2''(CT) emissions;
- the phosphorescence spectra of all molecules under study show a hipsochromatic shift i.e., if polarity of the solvent increases then λ_{max} decreases. This indicates that the phosphorescence bands stem from triplet (n, π^*) states [21]. In a particular solvent the maximum value of the phosphorescence band for all the studied components is roughly the same. Such a coincidence indicates that the phosphorescence spectra originate from the same chromophor i.e., from the benzoic moiety. This finding has its further explanation [22];
- for **III** and **IV** in polar solvents a weak emission from the TICT species occurs with $\lambda_{max} \cong 475$ nm (in Fig. 4(a) to [4](d) this band is plotted as a dotted line). The F_2''(CT) band at 77 K shows a blue shift in comparison with its λ_{max} value at room temperature.

4. Results of the fluorescence decay time measurements

4.1. Basis for the fluorescence decay time data analysis

The unusual emission of **III** and **IV**, noticed in these studies [14–16] can be explained by the following excited-state kinetic scheme

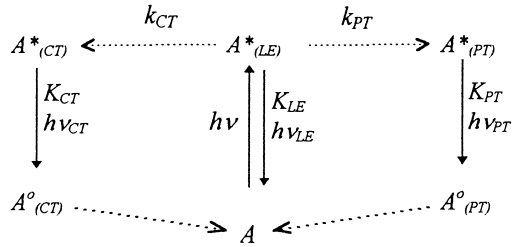

(1)

where $A^*_{(LE)}$, $A^*_{(PT)}$ and $A^*_{(CT)}$ denote molecules in the first excited state of the parent molecule, proton-transfer tautomers and TICT isomers, respectively. The $A^0_{(PT)}$ and $A^0_{(CT)}$ denote the equivalent molecules in the Franck–Condon ground states. The dashed lines represent radiationless transitions. The k_{PT}, k_{CT} parameters are the rate constants of proton-transfer tautomer and TICT isomer creation; K_{LE}, K_{PT} and K_{CT} are the deactivation constants of the molecules from the S_1(LE), S_1'(PT), S_1''(CT) states, respectively, and are equal to the sum of radiative, k^F, internal conversion, k^{IC}, and intersystem crossing rate constants, k^{ISC}, according to the equations:

$$K_{LE} = k^F_{LE} + k^{IC}_{LE} + k^{ISC}_{LE} = (\tau^F_{LE})^{-1} \quad (2a)$$

$$K_{PT} = k^F_{PT} + k^{IC}_{PT} + k^{ISC}_{PT} = (\tau^F_{PT})^{-1} \quad (2b)$$

$$K_{CT} = k^F_{CT} + k^{IC}_{CT} + k^{ISC}_{CT} = (\tau^F_{CT})^{-1} \quad (2c)$$

In the kinetic scheme above reversible proton-transfer and charge-transfer rate constants are omitted because of their supposed negligible values.

In order to confirm the validity of this scheme, apart from the above spectroscopic studies the fluorescence decay time measurements have been performed both for fluid and rigid solution.

According to kinetic scheme 1, after having excited fluorescent molecules with a δ-light pulse to the S_1(LE) states, the following rate equations should describe depopulation processes of the S_1(LE), S_1'(PT) and S_1''(CT) states:

$$\frac{d\left[A^*_{(LE)}\right]}{dt} = -(K_{LE} + k_{PT} + k_{CT})\left[A^*_{(LE)}\right] \quad (3a)$$

$$\frac{d\left[A^*_{(PT)}\right]}{dt} = k_{PT}\left[A^*_{(LE)}\right] - K_{PT}\left[A^*_{(PT)}\right] \quad (3b)$$

$$\frac{d\left[A^*_{(CT)}\right]}{dt} = k_{CT}\left[A^*_{(LE)}\right] - K_{CT}\left[A^*_{(CT)}\right] \quad (3c)$$

Solving the set of rate equations from (Eq. (3a)) to (Eq. (3c)), one can find that the intensity changes of the normal $I_{LE}(t)$, proton-transfer $I_{PT}(t)$, and charge-transfer $I_{CT}(t)$, fluorescence modes are described by mono- (Eq. (3a)) or double- (Eq. (3b)) and (Eq. (3c)) exponential functions [23]. In such conditions if one selects with an absorption filter the required fluorescence mode, a bi-exponential fluorescence decay should be observed for any

Table 1
The fluorescence decay times (in *ns*) of the molecules under study in various solvents and at various temperatures

Compound	Temperature (K)	Solvent	$\lambda_{ex}/\lambda_{obser}$ (nm)	τ_1/τ_2 (ns)	Relative weights
Benzamide I	296	MCH	266/F_1(LE) band	2.02 ± 0.06	1.00
	77	MCH	266/F_1(LE) band	3.00 ± 0.05	1.00
		EPA	266/F_1(LE) band	2.63 ± 0.05	1.00
N-methylbenzamide II	296	MCH	266/F_1(LE) band	0.072 ± 0.02/ 2.08 ± 0.04	0.80/0.20
	77	MCH	266/F_1(LE) band	0.075 ± 0.02/1.95 ± 0.05	0.70/0.30
		EPA	266/F_1(LE) band	0.085 ± 0.02/2.00 ± 0.04	0.80/0.20
N-phenylbenzamide (benzanilide) III	296	MCH	266/F_2'(PT) and F_2''(CT) bands	0.75 ± 0.01/1.45 ± 0.04	0.80/0.20
		MCH	300/440	0.79 ± 0.04	1.00
			300/520	0.92 ± 0.04	1.00
		IP/EE	266/F_1(LE) and F_2''(CT) bands	0.035 ± 0.01/1.25 ± 0.04	0.40/0.60
	168	MCH	300/400	2.52 ± 0.04	1.00
	77	MCH	266/400	2.95 ± 0.05	1.00
		EPA	266/F_1(LE) and F_2''(CT) bands	0.090 ± 0.01/ 1.65 ± 0.05	0.60/0.40
		IP/EE	266/F_1(LE) and F_2''(CT) bands	0.054 ± 0.01/ 2.13 ± 0.05	0.80/0.20
N-methylphenylbenzamide-(*N*-methylbenzanilide) IV	296	MCH	285/460	1.62 ± 0.06	1.00
			285/510	1.71 ± 0.06	1.00
		MCH	266/ F_2''(CT) band	1.70 ± 0.05	1.00
		IP/EE	266/F_1(LE) and F_2''(CT) bands	0.095 ± 0.01/1.30 ± 0.05	0.35/0.65
	168	MCH	285/475	1.90 ± 0.06	1.00
	77	MCH	266/F_2''(CT) band	2.05 ± 0.07	1.00
		EPA	266/F_1(LE) and F_2''(CT) bands	0.107 ± 0.01/ 1.70 ± 0.05	0.65/0.35
		IP/EE	266/F_1(LE) and F_2''(CT) bands	0.135 ± 0.01/ 2.15 ± 0.05	0.70/0.34

wavelength of the F_2 emission band of **IV**. In the case of **III** in 296 K, where the bands of the two fluorescence modes overlap (see Fig. 3(a)), the fluorescence decay curve is described by the formula being the sum of the solutions of (Eq. (3b)) and (Eq. (3c)).

Therefore, all experimental data were analysed using mono- and double-exponential fitting functions employing the complete (taking into account the profile of the excitation pulse) iterative deconvolution technique as described in [19]. Table 1 assembles the fluorescence decay time values for one of the above fitting procedures i.e., that one which gives the χ^2 value closer to one.

4.2. Benzamide and N-methylbenzamide

From the spectroscopic studies of **I** and **II** one expects that the fluorescence decay curves should be fitted by a mono-exponential model function. The τ_F data (see Table 1) of the fluorescence decay of **I** obtained at 296 and 77 K meet the above expectations. However, the fluorescence decay of *N*-methylbenzamide can be fitted satisfactory by a bi-exponential model function only. This indicates that the fluorescence emission of **I** appears from a species of one kind, whereas in the case of **II** two kinds of excited species (*cis*- and *trans*- tautomers) take part in the emission at room temperature and at 77 K. It has to be noticed that in the case of **II** the relative weights of the fast (ps region) and slow (ns region) decaying components are not sensitive to changes of temperature. The τ_2 (the slowly decaying component) is almost equal to the fluorescence decay time of **I**.

4.3. N-phenylbenzamide and N,N'-methylphenylbenzamide

The spectroscopic studies of molecules **III** and **IV** indicate that the fluorescence intensity changes of the normal $I_{LE}(t)$, charge-transfer $I_{CT}(t)$ and proton-transfer $I_{PT}(t)$, emissions might be described by mono- or multi-exponential model functions. At room temperature the intensity of the normal fluorescence is too weak to determine its decay time so that the fluorescence decay of the F_2 emission has been recorded only. At low temperature the intensity of the F_1(LE) band increases, and then it is possible to perform its decay time measurements.

As it was mentioned the F_2 band of **III** at 296 K in MCH solution was supposed to consist of the two components (Fig. 3(a), dash-dot lines). In order to confirm the dual nature of F_2 we have determined the fluorescence decay times in two wavelength regions i.e., at $\lambda_1 = 440$ nm and $\lambda_2 = 520$ nm. The decay times $\tau(\lambda_1)$ and $\tau(\lambda_2)$ equal to 0.79 ± 0.04 ns and 0.92 ± 0.04 ns, respectively. The difference between them ($\Delta\tau_{1/2} = 0.13$ ns) exceeds the error limit of τ determination. When one fits the experimental data points of the decay curve of the total F_2 band by a bi-exponential fitting function, the τ_1 and τ_2 values equal to 0.75 ns and 1.45 ns, respectively. The two decay modes participate 67% and 33% in the total decay. This result is in a very good agreement with the value obtained by the decomposition of the F_2 band into two bands (cf. section 3). It must be noticed that the fitting procedure by mono- and bi-exponential function give an equally good fit (Fig. 5). As it can be seen in Fig. 4(c) the *N*-phenylbenzamide emission

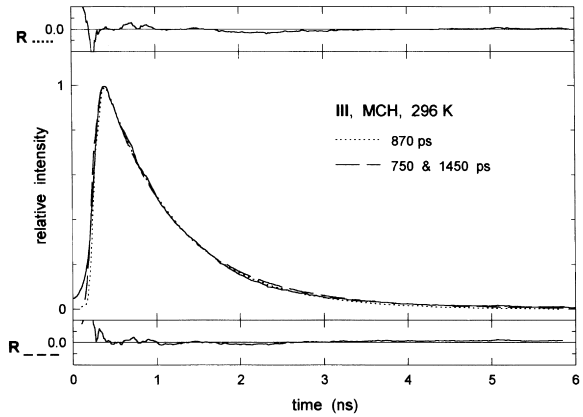

Fig. 5. The fluorescence decay curve of *N*-phenylbenzamide in MCH measured at 296 K; $\lambda_{ex} = 266$ nm. The experimental data (———) have been fitted with (. . .) a mono-exponential and (–) a bi-exponential model function. The relative weights of the 'fast' ($\tau_1 = 750$ ps) and the 'slow' ($\tau_2 = 1450$ ps) components are 0.8 and 0.2, respectively.

spectrum in IP/EE mixture at room temperature exhibit the F_1(LE) and F_2''(CT) bands. Their decay times equal to 35 ps and 1.25 ns, respectively.

The fluorescence emission of **III** in MCH at 77 K consists of the very weak F_1(LE) ($\lambda_{max} = 314$ nm) and the intensive F_{agr} ($\lambda_{max} = 420$ nm) bands. It means that the very weak F_1(LE) emission do not influence the fluorescence decay of *N*-phenylbenzamide aggregates. Therefore, the fluorescence decay is described by a mono-exponential fitting function. The decay time of the aggregates equal to 2.95 ± 0.05 ns. The same value (3 ns) has been measured by O'Connel et al. [7].

The fluorescence emission of **III** in rigid EPA and IP/EE mixtures comprise two bands: F_1(LE) and F_2''(CT). Their fluorescence decay times equal to 90 and 54 ps for the F_1(LE) emission and to 1.65 and 2.13 ns for the TICT fluorescence band, respectively.

Since *N*,*N*′-methylphenylbenzamide (**IV**) is capable of exhibiting the TICT type behaviour in all the solutions used, it always possesses two fluorescence bands i.e., the F_1(LE) and F_2''(CT) ones. The decay times of those fluorescence modes are in the region of about 100 ps (for the F_1(LE) emission) and about 2 ns (for the F_2''(CT) emission) varying with the change of temperature and solvent. The exact data are given in Table 1. It must be noticed that the τ values for **IV** in MCH determined for different sections of the F_2''(CT) band do not depend on λ, contrary to *N*-phenylbenzamide.

5. Conclusions

The fluorescence spectra of **I** and **II** obtained at room and low temperatures consist of one broad band without any noticeable vibrational structure. The fluorescence decay time data indicate that the radiation of **I** derives from one kind of species, whereas in the case of **II** from the *trans*- and the *cis*- tautomeric forms. The decay times of the tautomeric forms differ.

The F_2 fluorescence decay curve of **III** obtained at 296 K at different emission wavelengths can be fitted by a single exponential function with different decay constants. Nevertheless, a bi-exponential fit gives equally good result with τ_1 and τ_2 values not differing from that obtained for total, F_2'(PT) and F_2''(CT), band measurements. This result gives additional support to the statement that the F_2 band of **III** in MCH at 296 K consists of two transitions i.e., F_2'(PT) and F_2''(CT) bands characterised by different decay constants. The F_2'(PT) and F_2''(CT) band participation in the total F_2 band agree with the results obtained on the grounds of fluorescence decay time measurements.

The fluorescence spectra of **III** and **IV** in glasses differ from those obtained in fluid solutions. *N*-phenylbenzamide only in MCH rigid glass has a new band (onset 350 nm, $\lambda_{max} = 420$ nm), whereas in IP/EE and EPA glasses the F_1(LE) at about 330 nm and F_2''(CT) at ≅470 nm bands remain. The fluorescence emission changes of **III** at room and low temperatures are reflected in the determined decay times. We suppose that the new fluorescence band at 420 nm of molecule **III** in MCH rigid solutions derives from its dipolar aggregates [8,13,20]. The F_2 fluorescence spectra of **IV** in MCH and IP/EE glasses at 77 K possess the F_1(LE) and F_2''(CT) bands with λ_{max} at 320 nm and 500 nm. The decay curve of the total emission is described by the bi-exponential function.

The short fluorescence decay times of the F_1(LE) bands of **III** and **IV** indicate that the k_{PT} and k_{CT} rate constants are large and consequently, the two depopulation ways of the S_1(LE) state are very efficient. Our results show that the TICT deactivation mechanism is not the dominant one. This finding shows that in hydrocarbon solutions like MCH, the hypotheses of Azumaya et al. [17] and that of Tang et al. [8] are only partially correct.

The phosphorescence spectra of the molecules studied yield blurred vibrational structure. The λ_{max} values of the phosphorescence bands depend on the polarity of the frozen solvents. The blue shift noticed for λ_{max}(Ph) alongwith increasing solvent polarity and observed marked vibrational structure of the phosphorescence band in polar solvents indicate that the T_1(LE) states of the molecules under study have a mixed $n,\pi^*-\pi,\pi^*$ origin [7,16,17]. The λ_{max} value of the phosphorescence spectra of the compounds in question are equal if measured in the same kind of rigid glasses. It indicates that the benzoic moiety of the molecules is responsible for the T_1(LE) → S_0 emission. The phosphorescence band intensity of compounds **I** and **III** is greater than that of the *N*-methyl substituted compounds (**II** and **IV**). This finding agrees with the result of our earlier papers [22,24].

Acknowledgements

This work was partly supported by Grand of the University of Gdańsk BW 5200-5-0200-8 and the Pedagogical University at Słupsk. We are thankful to Prof. E. Hilinski,

Department of Chemistry, Florida State University and Prof. W. Rettig, Department of Chemistry, Humboldt University at Berlin for making accessible the fluorescence decay time measurements.

References

[1] A.V. Belotsvetov, V.I. Danilova, E.V. Borisov, M.K. Verzilina, T.A. Savelova, L.V. Gorchakov, Zhurnal Fizicheskoii Khimii 50 (1976) 1941–1945.
[2] V.A. Kosobutskii, G.I. Kagan, V.K. Belyakov, O.G. Tarakanov, Zhurnal Fizicheskoii Khimii 12 (1971) 822–830.
[3] T.A. Modro, K. Yates, F. Beautays, Can. J. Chem. 55 (1977) 3050–3057.
[4] D.J. Carlsson, L.H. Gan, D.M. Wiles, Can. J. Chem. 53 (1975) 2337–2344.
[5] G.I. Sarapulovo, N.N. Chipanina, L.Ł. Volkova, R.G. Sultangareev, I.T. Yushmanova, N.A. Khlopenko, V.A. Lopyrev, Yu.L. Frolov, Izvestiya Akademii Nauk SSSR, Seriya Khimicheskaya 10 (1984) 2255–2259.
[6] J.T. Edward, Sin Cheong Wong, J. Am. Chem. Soc. 99 (1977) 4229–4232.
[7] E.J. O'Connell, M. Delamauro Jr., J. Lrwin, J. Photochem. Photobiol. 14 (1971) 189–195.
[8] G.Q. Tang, J. MacInnis, M. Kasha, J. Am. Chem. Soc. 109 (1987) 2531–2533.
[9] L.S. Prabhumirashi, D.K. Narayanan Kietty, Anjali S. Bhide, Spectrochemia Acta 39 A (1983) 663–668.
[10] CH.L. Perrin, E.R. Johnson, J. Am. Chem. Soc. 103 (1981) 4698–4703.
[11] A.G. Redfield, S. Waelder, J. Am. Chem. Soc. 101 (1979) 6151–6162.
[12] Aboul-Fetouh E. Mourad, Spectrochimica Acta 44 A (1988) 53–56.
[13] J. Heldt, J. Photochem. Photobiol. 60 (1991) 183–191.
[14] J. Heldt, D. Gormin, M. Kasha, J. Am. Chem. Soc. 110 (1988) 8255–8256.
[15] J. Heldt, D. Gormin, M. Kasha, Chem. Phys. Lett. 150 (1988) 433–436.
[16] J. Heldt, M. Kasha, J. Mol. Liquids 41 (1988) 305–313.
[17] I. Azumaya, H. Kagechika, Y. Fujiwara, M. Itoh, K. Yamaquchi, K. Shudo, J. Am. Chem. Soc. 113 (1991) 2833–2838.
[18] W. Rettig, M. Vogel, E. Lippert, H. Otto, Chem. Phys. 103 (1986) 381–390.
[19] J.A. Schidt, E.F. Hilinski, Rev. Sci. Instrum. 60 (1989) 2902–2914.
[20] E. Lipczyńska-Kochany, Some New Aspects of Hydroxamic Acids Chemistry, Wydawnictwa Politechniki Warszawskiej, Warszawa, 1988.
[21] N.J. Turro, Modern Molecular Photochemistry, The Benjamin/Cummings Publication, Inc. Menlo Park, California (1978) Chapter 5.
[22] M. Kasha, J. Heldt, D. Gormin, J. Phys. Chem. 99 (1995) 7281–7284.
[23] W.R. Laws, L. Brand, J. Phys. Chem. 83 (1979) 795–802.
[24] D. Gormin, J. Heldt, M. Kasha, J. Phys. Chem. 94 (1990) 1185–1189.